We are IntechOpen, the world's leading publisher of Open Access books Built by scientists, for scientists

6,000
Open access books available

148,000
International authors and editors

185M
Downloads

Our authors are among the

154
Countries delivered to

TOP 1%
most cited scientists

12.2%
Contributors from top 500 universities

CLARIVATE ANALYTICS
BOOK CITATION INDEX
INDEXED

WEB OF SCIENCE™

Selection of our books indexed in the Book Citation Index
in Web of Science™ Core Collection (BKCI)

Interested in publishing with us?
Contact book.department@intechopen.com

Chapter

Sugar Cane Products as a Sustainable Construction Material. Case Study: Thermophysical Properties of a Corncob and Cane Bagasse Ash Panel

Rafael Alavéz-Ramírez, Fernando Chiñas-Castillo,

Magdaleno Caballero-Caballero,

Valentín Juventino Morales-Domínguez,

Margarito Ortiz-Guzmán, Maria Eugenia Silva-Rivera,

Roberto Candido Jimenez-Piñon and Angel Ramos-Alonso

Abstract

Climate change is currently an issue that worries governments and society due to its threat. It is essential to implement efficient materials with low energy consumption in construction. This work shows the use of sugarcane products in the Mexican construction sector, aiming to mitigate the impact of energy wasting. As a case study, the analysis of thermophysical properties of a light mortar panel based on cane bagasse ash and corncob is presented. The experimental thermal properties of a hybrid panel system composed of cane bagasse ash, corncob, and lime were characterized. A sandwich-type construction component was made with two outer panels of reinforced mortar and between the panel of cane and corncob bagasse ash. Measurements of the surface temperatures of the system were conducted to determine the decrement factor and thermal lag, and the results were compared to other construction systems. The decremental factor and thermal lag were 0.19 (a reduction of 82%) and 6:03 h (an increment of 2400%) compared to the control panel of ferrocement only. These results are significant because the panel prepared limits the heat flow in peak hours when high temperatures reach their maximum values. This composite panel can provide an ecological alternative for energy-saving and thermal comfort and help fight climate change.

Keywords: cane, corncob, bagasse ash, thermal properties, insulation

1. Introduction

Due to climate change, governments have become more aware of the need to save energy and provide comfort in buildings. In this context, it is essential to develop and implement bioclimatic architectural systems that reduce energy consumption without affecting the thermal comfort of the building [1]. However, it is well known that most modern buildings and houses do not adapt to changing climatic conditions. The results are energy waste, health problems, and severe environmental effects. According to Wegertseder [2], the residential sector is responsible for 40% of the planet's emissions. Forty percent of greenhouse gas (GHG) emissions and one-third of black carbon emissions are from construction industries [3, 4].

On the other hand, green building analysts predicted that, by 2030, the building and construction sectors would produce more than 40 billion tons of carbon emissions [5, 6]. Imported commercial materials such as polyurethane-based insulating foams and polystyrene used to insulate the building negatively affect the ecological environment from production to disposal as waste material. The bioclimatic design provides criteria in buildings to help reduce energy demands and pollutant emissions into the atmosphere. The thermophysical characteristics of building materials are essential in minimizing thermal gains by conduction and radiation and obtaining thermal comfort conditions and energy savings. That is one of the most immediate ways to significantly reduce emissions [7] and up to 30% of energy consumption [8].

Thermal inertia is a necessary thermophysical property for extreme climates with significant thermal oscillations during the day and night. Thermal inertia represents the ability of a material to conduct and store heat, which is related to thermal conductivity and volumetric heat capacity. In contrast, heat transfer in the building is related to how fast or slow the interior temperatures reach the exterior temperature. Researchers are interested in developing composite materials with natural fibers, which generate thermal lag when combined with thermal inertia [9–15].

Sugar cane is a grass plant, and its stalk is fibrous. It is cultivated in several countries; It becomes an agricultural residue once the juice is extracted. The sugarcane bagasse has been used in thermal and acoustic insulation. The different procedures used to extract fibers can influence the chemical composition and fiber structure [16]. The sugarcane bagasse fiber surface can be changed to increase interfacial interactions considering the environmental criteria and produce functional components from biodegradable wastes [17]. The thermal conductivity of sugarcane bagasse fiber as an insulating material has also been investigated [18]. The results showed a thermal conductivity of 0.04610 w/m·K in the average temperature range of 15.6–32°C. Aminudin [19] investigated the improvement of cement bricks by 10% weight of sugarcane bagasse fiber, decreasing thermal conductivity to 0.62 w/m·K. Some studies report that the chemical composition is affected by fiber age, harvesting method, and climatic conditions such as cellulose, hemicellulose, lignin, and sugar ash [20].

Standard ASTM 618–00 defines pozzolans as "siliceous or alumino-siliceous materials which have little or no cementitious value, but when finely divided, and in the presence of water, react chemically with calcium hydroxide $Ca(OH)_2$ at room temperature to form compounds with cementitious properties". Chemical, physical and mechanical methods can be applied to characterize the pozzolanic reactivity of a material. The mechanical methods assess the role of the pozzolanic reaction in developing mechanical compressive strength in pozzolan-containing mortars and cement concretes. The pozzolanic reactivity indicates the pozzolan-lime reaction determined

by several methods [21]. Studies such as the one conducted by [22] have shown that these agricultural waste by-products contain high pozzolanic reactivity. The main components that govern the reactivity of a pozzolan are (SiO_2, Al_2O_3, Fe_2O_3, and CaO). Payá [23] evaluated the efficiency of two siliceous pozzolans, silica fume (SF) and rice husk ash (RHA), and a metakaolin silico-aluminous pozzolan MK. The results showed the high reactivity of these materials acting as pozzolans when combined with lime and the apparent dependence on the water/cement ratio of the mix and curing time.

When sugarcane bagasse is burned, sugarcane bagasse ash (SCBA), a mineral residue rich in silica and alumina, is produced. Its structure depends on the combustion temperature [24]. This product can be used as a pozzolan in cement-based pastes. Several authors [25–28] have found that using SCBA as a partial replacement for portland cement improves the durability and mechanical properties of cementitious materials. The benefits developed by SCBA are due to physical and chemical effects linked to its ability to provide amorphous silica that will react with Ca $(OH)_2$ in water during cement hydration. SCBA is usually obtained under uncontrolled burning conditions [27]. Thus, the ash may contain black particles due to the presence of carbon and crystalline silica when burning occurs at high temperatures (above 800°C) or for prolonged times. The ash quality can be improved by controlling temperature, heating rate, soaking time, and atmosphere, as previously reported for the highly pozzolanic rice husk ash (RHA) [29]. On the other hand, carbon and unburned material can lower the pozzolanic activity of sugarcane bagasse ash [25]. Particle size, calcination temperature, amorphous structure, and chemical composition all affect the pozzolanic activity of bagasse ash [30–32]. The calcination temperature at 600°C is essential for producing sugarcane bagasse ash with pozzolanic activity [31]. It presents amorphous silica, low carbon content, and high specific surface area [23, 27]. Laboratory tests on the pozzolanic reactivity of Cuban sugar cane wastes (straw and bagasse) revealed that the ashes have intense pozzolanic activity and can be used as active additives in cement manufacture [32].

1.1 Recent reserch on sugarcane bagasse ash

This section highlights recent research using sugarcane bagasse ash as a pozzolanic material. Nengsen Wu [33] developed ultra-high performance green concrete (UHPC) with sugarcane bagasse ash (SCBA) as a replacement for cement. SCBA's effects on UHPC flowability, setting time, compressive strength, and shrinkage were investigated. The results showed that using SCBA in UHPC as a cement replacement maintains compressive strength, improves workability, and reduces shrinkage of the UHPC paste. Autogenous shrinkage was reduced by 24.48%, but compressive strength was nearly identical. Yadav [34] conducted an experimental investigation to demonstrate the effectiveness, availability, and cheap cost of geopolymers generated from mechanical milled sugarcane bagasse ash and metakaolin. According to this investigation, the sugarcane bagasse ash and metakaolin need mechanical and chemical treatment to increase their pozzolanic reactivity. Mehrzad et al. [35] fabricated and tested fibrous sugarcane bagasse (SBW) samples with different densities, thicknesses, surface morphology, and tensile properties. They conclude that sugarcane bagasse fiber samples can be a new sustainable building material in terms of thermal and acoustic qualities. Brito [36] studied sugarcane and bamboo-based particleboards. Three proportions of blends (25, 50, and 75%) were adopted for particle boards. The boards

made with 75% bamboo particles and 25% sugarcane bagasse particles achieved the values required by the standard for thickness swelling in 24 h.

Gharieb [37] studied the use of carbonation and lime wastes from sugar beets (CLR) to partially replace cement as a cementitious material. The optimal level of CLR was 5%, which increased compressive strength and microstructure. The results confirmed that it is possible to use CLR as a cementitious material. Jagadesh [38] explored the use of Processed Sugar Cane Bagasse Ash (PSCBA) in various proportions in cementitious mortar. Portland cement with PSCBA lowers energy usage, reduces domestic gas emissions, and enhances cement characteristics. It was observed that cement mortar's mechanical and fracture properties with 10% substitution of PSCBA in ordinary Portland cement show improved properties. Jittin & Bahurudeen [39] examined the rheological performance and compressive strength of sugarcane bagasse and rice husk ash using a ternary-based hybrid cementitious system. The yield strength, plastic viscosity, and consistency index increase with added sugarcane bagasse ash and rice husk ash. The highest compressive strength was observed for ternary mixed concrete with 10% bagasse ash and 5% rice husk ash, followed by binary concrete mixed with 20% bagasse ash. SCBA as a supplementary cementitious material (SCM) and supplemental filler material (SFM) for usage in the construction sector has awakened the interest of researchers. Processed SCBA has improved characteristics compared to its unprocessed counterpart, with an optimum replacement of 20% [40]. Therefore, it is very effective as a supplementary binder and filler material.

Souza [41] investigated the development of lightweight mortars from sintering SBA. Two different SBA were evaluated; one was produced in a ball mill and the other in a knife mill. The findings show that lightweight aggregates based on SBA and RC binary mixtures can be produced in a wide range of particle densities from 1.03 to 1.67 g/cm^3. Subedi [42] investigated the feasibility of using high contents of co-processed sugarcane bagasse ash (PBA) as a partial cement replacement for the development of engineered cementitious composites (ECC) with a 1.5% volume of polyvinyl alcohol (PVA) fibers. The results showed that the workability of the mixtures decreased with increasing PBA content. Furthermore, adding PBA decreased compressive strength up to 39% and increased surface resistivity, where composites outperformed control composites. The use of PBA produced a reduction in the crack tip.

Klathae [43] investigated bagasse ash (BA) from processed sugar mills. HVGBA concrete compressive strength, tensile strength, elastic modulus, and drying shrinkage were investigated [43, 44]. The results showed that using HVGBA could reduce the maximum temperature rise between 8 and 19°C of the control concrete (CT). All concrete incorporating HVGBA with different LOI had higher drying and shrinkage than CT concrete, increasing the LOI and cement replacement rate. Barbosa [45] examined the effect of SCBA with various chemical and mineralogical compositions on paste hydration, compressive strength, and autogenous shrinkage of mortars. SCBA samples with high levels of amorphous silica-rich, fewer pollutants, and a high specific surface area behaved like RHA, with effects on hydration. Combined SCBA mortars, regardless of SCBA type, caused an increase in compressive strength. However, only the SCBA plus pozzolanic mortar was comparable to RHA.

Athira and Bahurudeen [46] compared the microstructure of processed and received rice straw ash to SCBA. Microstructural analysis revealed that rice straw ash and SCBA are made of phytoliths, dumbbell-shaped silica storage structures. Rice straw ash is richer in phytoliths than SCBA; however, the prismatic structures in

SCBA are absent in rice straw ash. It is found that the yield strength and viscosity of the cement paste increase with the addition of rice straw.

Klathae [44] formally demonstrated that SCBA with proper particle size is an excellent pozzolanic material for concrete durability. They investigated high-strength concrete (HSC) with a high volume of sugarcane bagasse ash (HVSCBA). The results showed that the 28-day compressive strength of the binary and ternary binders HSC could be developed to meet the requirement of 55 MPa.

The following case study shows the thermal properties of a biodegradable hybrid panel based on a lightweight mortar combining sugarcane bagasse ash, corn stover, and lime. SCBA was combined with lime and generated a binder material according to the standard ASTM 618–00. A sandwich construction component was made with panels, two outer layers of reinforced mortar, and the SCBA and corncob panel (2F + POCE) in the middle. Measurements of the surface temperatures of the system were conducted to determine the thermal damping and thermal lag. These results were compared to other construction systems.

2. Case study: THERMOPHYSICAL properties of a sugarcane bagasse ash and corncob-based panel

2.1 The climate of Oaxaca city and bioclimatic strategies

The city of Oaxaca is located in the southeast of the Mexican Republic; its bioclimate is temperate [47]. Summers are humid along the eastern lowlands and present an average daytime temperature ranging from medium-low to medium-high 9 to 34°C. It has an altitude of 1550 meters above sea level and geographical coordinates of 17°04′04"N latitude, 96°43′12"W longitude. This place exhibits moderate relative humidity and summer rains as classified by Köppen [48]. Winds constantly move north to south, and solar radiation is intense on clear days. **Figure 1** summarizes the climatic data for the locality according to average values for the last decade from the National Meteorological Service (SMN). However, when the range of annual oscillation is more than 14°C, it is considered very extreme, according to Köppen-García [49].

2.2 Materials used in the hybrid panel

The SCBA used to elaborate the biodegradable hybrid panel was obtained directly from a sugarcane mill in Ciénega, Zimatlán de Álvarez Oaxaca, 20 minutes away from the capital city of Oaxaca-Mexico. **Table 1** shows a typical chemical composition of sugarcane bagasse [52]. The ash selected for this study is derived from making sugar cane, where the sugar cane juice must be squeezed, and the bagasse obtained is used to burn in the oven. The temperatures reached inside the oven are above 700°C.

The ashes obtained from the furnace's interior were homogenized by quartering based on the Mexican Official Standard NOM-AA-61. The SCBA particles were washed and exposed to the sun for 48 hours. Selected SCBA and corn stover material were taken to the drying area at CIIDIR IPN Oaxaca. The corncob was obtained from the local market. The material used as a binder in the panel matrix was pine resin obtained from the town of Ixtlán Oaxaca, located 30 minutes from the capital city of Oaxaca-Mexico.

	Annual	March
Mean maximum	30.4	32.9
Mean minimum	13.6	12.9
Mean	22	22.9
Minimum temperature	7.0	9.7
Thermal oscillation	16.8	20
Mean wind speed	1.8	1.9
Horizontal global radiation	682.5	783
Relative humidity	65.6	55
Heating degree days (18°C)	3033.8	288.3
Cooling degree days (20°C)	- 1270.2	- 176.7

The geographic location of Oaxaca city

Figure 1.
Average climatic data and location for the city of Oaxaca, Mexico.

Cellulose (%)	Hemicellulose (%)	Lignin (%)	Ash (%)	Extractives	References
51	30.10	12.50	2	—	[50]
43.8	28.60	23.50	1.30	—	[51]

Table 1.
Chemical composition of sugar cane bagasse.

Granulometry tests were carried out on the SCBA. The sugar cane husk determines the percentage of fines in the SCBA. It ensures its pozzolanic reaction with the calcium hydroxide to determine the particle size of the husk to be used in the hybrid panel. The particle size test was carried out by adopting the recommendations of the manual M.MMP.1.103, disaggregated drying, and quartering of samples. The granulometry of both materials was carried out in a WS TYLER Sieve ROTAP machine Model RX-29 for 5 minutes. The passage of the SCBA material was done through different meshes No. 4 (4.76 mm), No. 10 (2.00 mm), No. 20 (0.84 mm), No. 40 (0.42 mm), No. 60 (0.25 mm), No. 100 (0.149 mm) and No. 200 (0.074 mm) to obtain the retained mass in each mesh, and calculate its percentage. The material that passed mesh # 200 was the percentage of fines.

In order to determine the granulometry of the corncob, it was decided to use the corncob particles retained in mesh No. 4 (4.76 mm). It was mixed with the SCBA as a cementitious agent.

	CAL	SCBA
Element/compound	%	%
Al_2O_3	N.D	9.92
CaO	68.63	2.59
Fe	0.4	2.7
Fe_2O_3	0.14	2.32
FeO	0.39	1.39
K_2O	0.22	2.1
MgO	0.42	1.44
MnO	ND	0.14
Na_2O	ND	0.23
P_2O_5	ND	0.9
PXC at 950°C	29.84	24.15
SiO_2	0.31	51.66
TiO_2	ND	0.74
Density (kg/m^3)	21.97	21.48
ND = Undetected		

Table 2.
Chemical properties of lime and SCBA.

Table 2 summarizes the chemical properties of the SCBA and lime. It was observed that 51.66% of silicon oxide was present in the SCBA, which allowed it to react with the hydroxide in lime with 68.63%.

Finally, the reinforced mortar (ferrocement) is the construction element used to cover the biodegradable panel as a sandwich type. Ferrocement is a construction material composed of reinforced concrete and several layers of reinforcing mesh, electro-welded mesh, and chicken wire, uniformly distributed throughout a cross-section (ACI 549R-93). A mortar rich in cement, sand, and water was used for its making. This material has a thickness of 0.025 m. It is characterized by its high strength and flexibility and is a low-cost material. The mortar used to make the ferrocement slab is a Portland cement type 1 from Cooperativa La Cruz Azul SCL that meets all the ASTM C-150-89 standard requirements. Natural sand, clean and free of organic substances, sieved with the # 8 (2.38) ASTM. The average grain size was 0.7 ± 0.145 mm. Water from the distribution network was taken to the locality to prepare the mixture. The mechanical properties of the mortar used in this study can be found in [53].

2.3 Preparation of test panels

A lightweight mortar made of SCBA, corncob, and lime was used as a base to elaborate the (2F + POCE) panels, whose mechanical properties were previously studied by the authors of the current chapter [54]. A lightweight mortar was also developed, taking advantage of the SCBA and lime characteristics to obtain a cementitious agent to stabilize the mixture. The SCBA and lime mixture was prepared manually; water was added until a uniform consistency was achieved. The specimens were compacted

manually with a wooden mallet. Finally, two panels of dimensions 1 m x 1 m long x 10 cm thick were made to determine the thermal damping properties and thermal conductivity. The specimens were left to dry for three weeks before their thermal properties were obtained. Finally, two 1 m x 1 m x 0.25 m thick ferrocement plates were fabricated to form the hybrid sandwich panel. The two ferrocement plates cover the plate filled with a 1 x 1 x 0.10 m thick waffle matrix, forming the composite panel. **Figure 2a** shows the panel with the sugarcane bagasse-lime-corncob ash matrix. **Figure 2b** shows the hybrid sandwich panel with two layers of reinforced mortar (2F + POCE).

2.4 Determination of decrement factor and thermal lag

In order to determine the damping and thermal retardation properties, first, the analysis date had to be defined. In doing so, the data of the highest solar radiation of the locality was considered, which corresponded to March (**Figure 3**); such data were obtained from the climatic normals for Oaxaca city (1980–2010) (SMN).
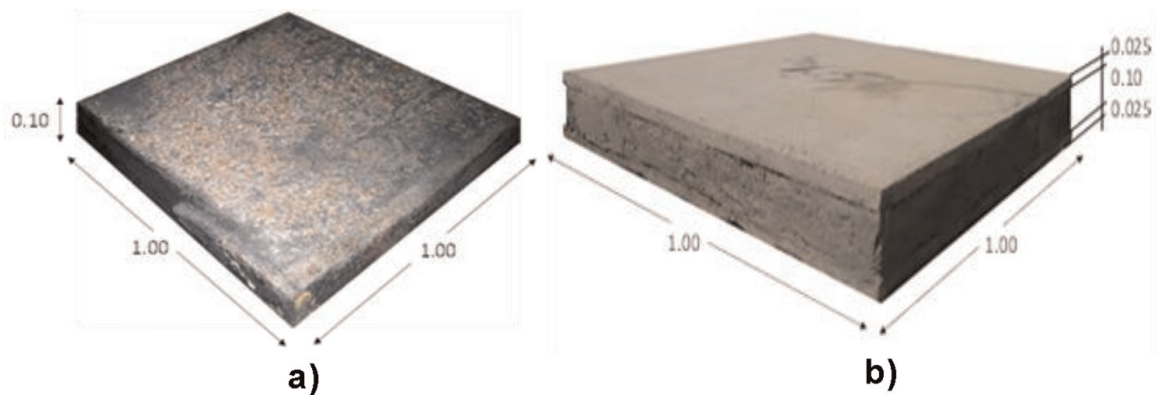
Figure 2.
Hybrid panel: a) cane bagasse ash-lime-corncob matrix, b) panel with two ferrocement plates and, in between, a panel with sugarcane bagasse-lime-corncob ash matrix.
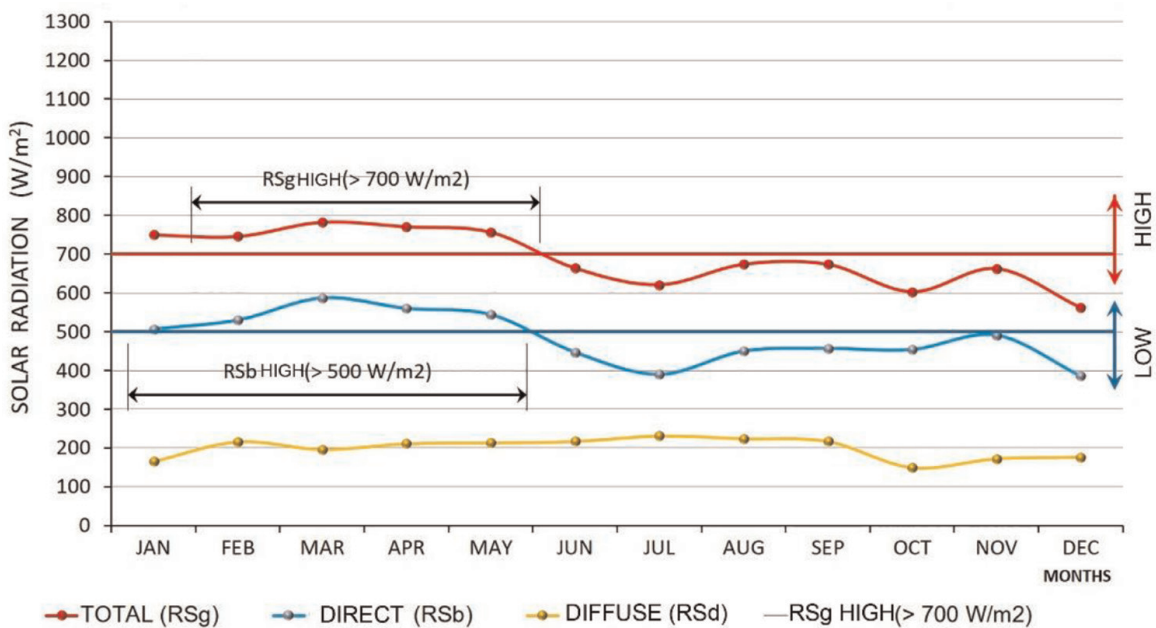

Figure 3.
Solar radiation for the city of Oaxaca.

Temperature measurements were made using five experimental chambers built for this purpose. Surface temperature measurements were carried out using 30 TMC6-HD Smart sensors (−40 to 100°C) connected to a 12-bit HOBO12 data logger system. It includes HOBOware software and a standard NIST calibration kit and stores 43,000 readings at a sampling rate of 1 s-18 h. **Figure 4** shows the placement of sensors in a thermal chamber; three were connected on the inner surface part of the specimens and three on the outer surface part of the specimens. The hobo was placed at 2.50 m inside a thermal shelter for outdoor air temperature recording to avoid direct solar radiation and allow cross ventilation.

The thermal properties of the proposed panel (2F + POCE) were compared to other construction elements built for that purpose, as shown in **Table 3**.

Figure 5a shows the placement of the different construction elements in the thermal chambers. It is worth mentioning that the thermal chambers were insulated on five sides. The upper part was left open to place the panel and allow direct solar radiation (**Figure 5b**).

2.5 Determination of thermal conductivity properties

Therm conductivity measurements were made on a homemade hot plate conductivimeter at CIIDIR IPN Oaxaca on the PO + CE panels utilized in this work [55]. This device is essentially a box with one side open, producing heat using an electric heating system. A Fiberfrax Blanket ceramic fiber quilt material resistance of 1260° is used to isolate the box's walls thermally. The conductivimeter is a device that
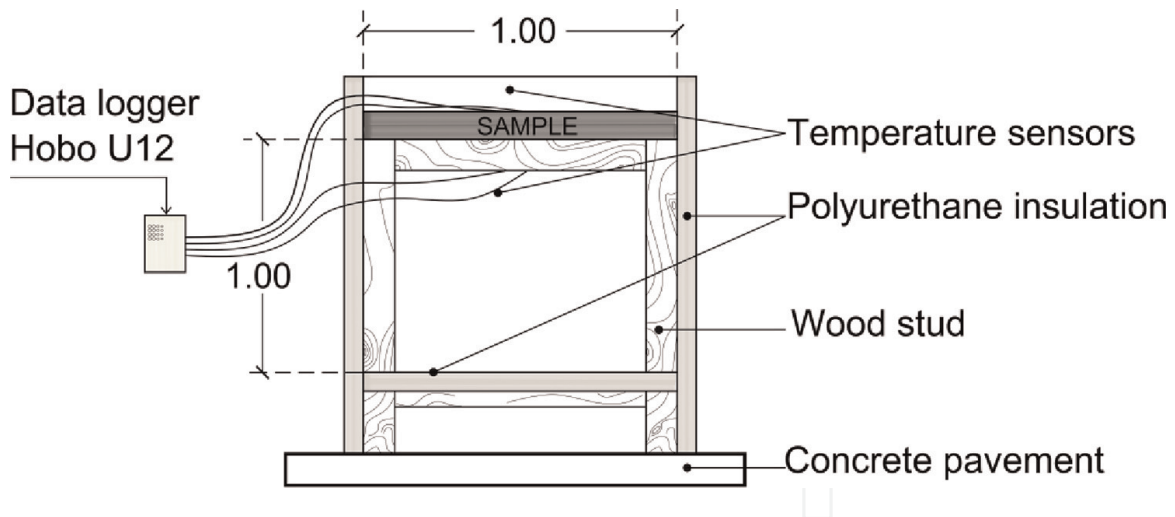

Figure 4.
Position of thermocouples, cross-section.

Wall panels	Dimensions (m)
Corncob Panel (PO + CE) (Matrix of SCBA, lime and corncob)	1,1,0.10
Ferrocement panel (LF)	1,1,0.025
Ferrocemento panels (0.025 m) + corncob panel as infill (2F + POCE) (0.10 m).	1,1,0.15
Concrete slab (CLC) (0.10 m)	1,1,0.10
Two ferrocement slabs + air (2F + A)	1,1,0.10

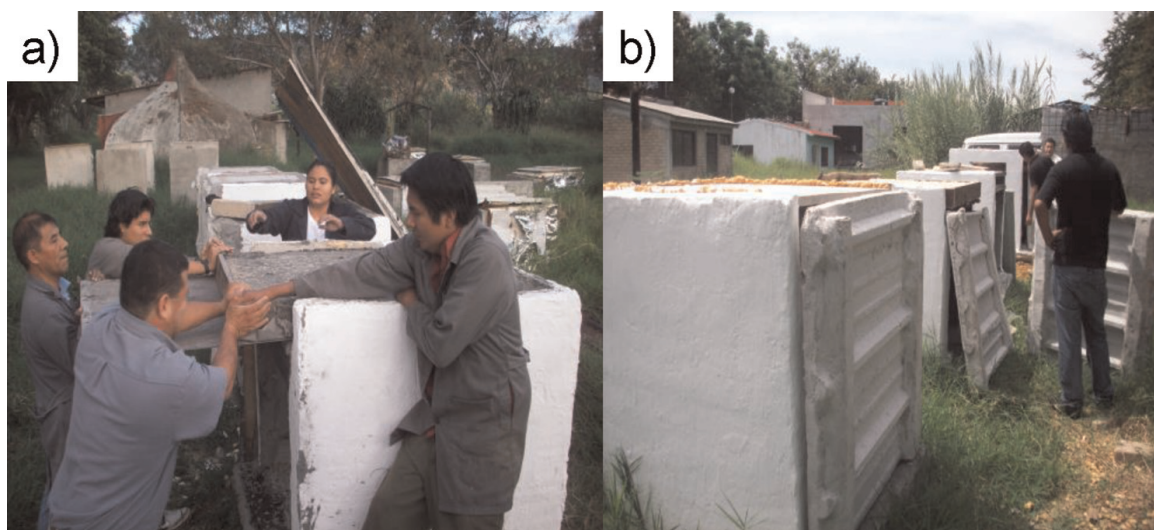**Table 3.**
Dimensions of panels.

Figure 5.
a) Cane bagasse ash panel placement; b) general view of the thermal chambers.

employs the steady-state conduction heat transfer concept and enables standard ASTM C 177 thermal conductivity determination using the equation:

$$k = \frac{Q}{A(\Delta T/L)} \tag{1}$$

where Q represents the rate of heat flow through the specimen in W, k represents its thermal conductivity in W/m K, ΔT represents the temperature differential through it in K, L represents its thickness in m, and A represents its cross-sectional area in m^2.

It is important to note that if the sample is a compound with pores or spaces where heat can be transmitted via conduction, radiation, or convection, k in Eq. (1) represents the apparent thermal conductivity.

The upper part of the conductivity meter is uncovered, where the panel was placed. Inside, there are installed 500 watts electrical resistance of stainless steel at 127 volts single-phase with dimensions of 1 m × 1 m with flexible terminals of 0.5 m in length, and high-temperature cable with a thickness of 4 mm.

The (2F + POCE) building component temperatures were recorded utilizing TC6-J type J thermocouples with a 2 m connector that supports temperatures of 0–800°C. These sensors are connected to a four-channel HOBO UX120-014 M data acquisition system, which stores the temperature information recorded by the thermocouples. **Figure 6** shows the flow diagram of the conductivity meter.

For this investigation, the PO + CE panel wall underwent five testing replicates. Temperature readings were obtained every 10 minutes. Only the range of steady state was taken to determine the mean temperature of each sensor after registered temperatures from the four sensors on the hot side and the four sensors on the cold side. The four sensors on the hot side were then averaged after that. The four sensors on the cold side underwent the same process. In order to determine the thermal conductivity of the panel wall tested, the temperature gradient was computed as the hot-side average temperature less than the cold-side average temperature. It should be noted that the mean temperature recorded in each sensor for each panel wall was calculated from more than 100 steady state points.
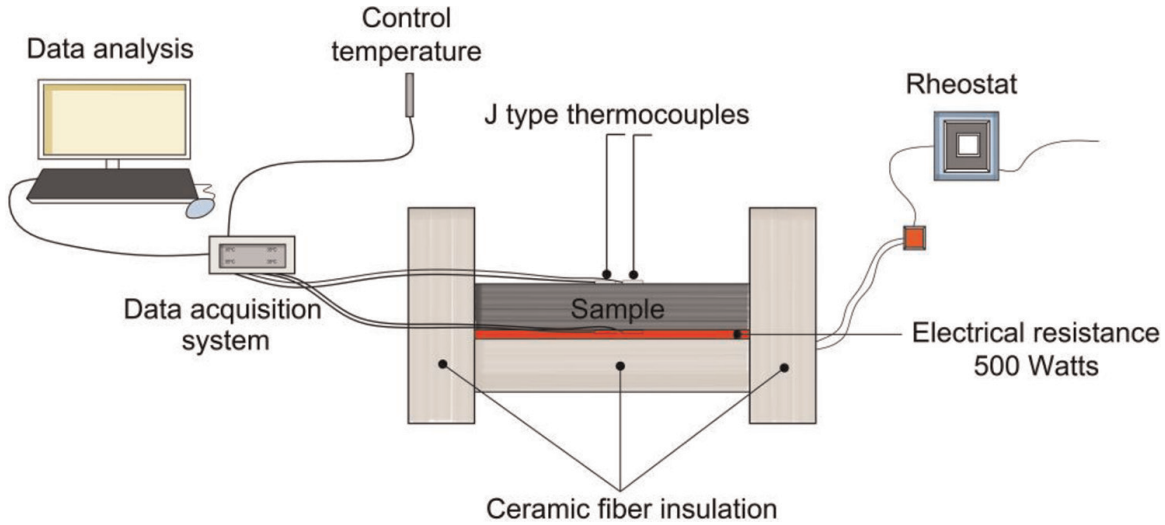
Figure 6.
Thermal conductivity test flow chart.

3. Analysis and discussion of results

3.1 Bioclimatic strategies for Oaxaca City

The results of the psychrometric chart (**Figure 7**) show that 77% of the time, people are thermally uncomfortable, and only 22.4% have thermal comfort conditions in the city of Oaxaca. It is observed that there are requirements of internal heating gain of 33.5%, thermal mass of 26.7%, shading of 22%, adaptive comfort ventilation of 18.6%, and forced ventilation of 21.9% for cooling. It is essential to mention that the percentage of internal heating gains (33.5%) is generated with the thermal mass
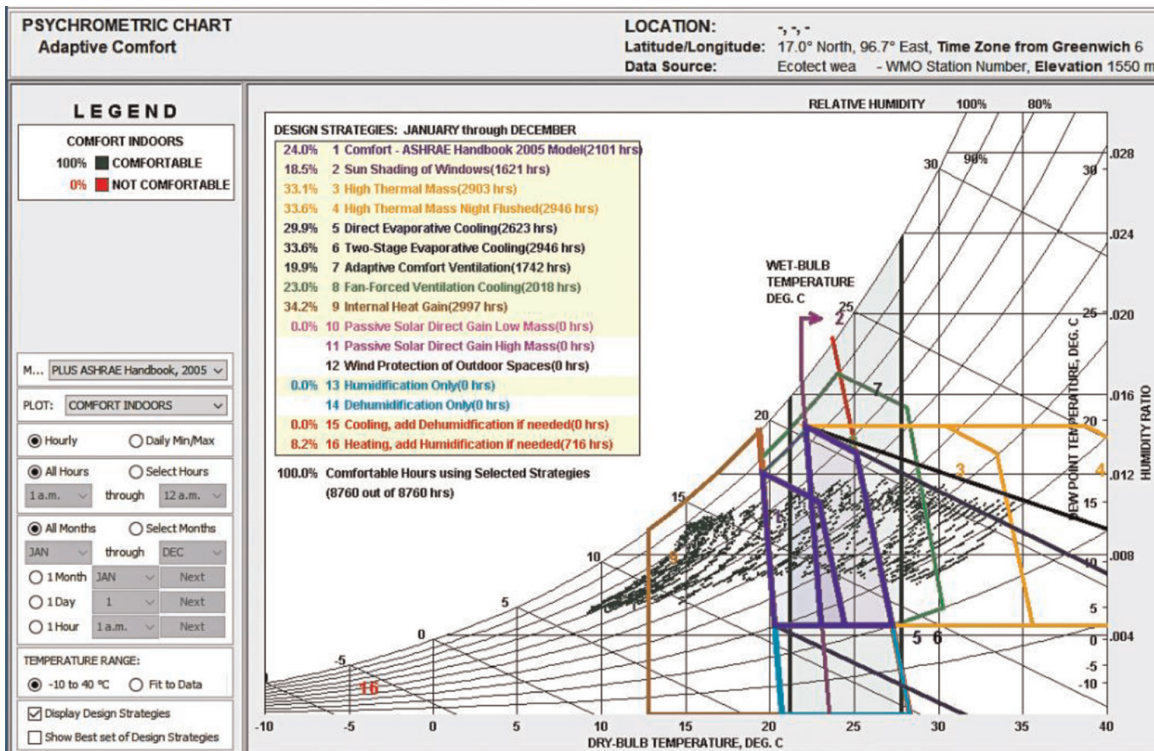

Figure 7.
Psychrometric chart for the city of Oaxaca.

because it can store the energy required during the day for passive heating. In this sense, the proposed hybrid panel can be a viable ecological alternative.

3.2 Results of thermal lag and decrement factor

Figure 8 presents the thermal measurements monitored inside the experimental cells taken in March. The analysis period was determined from March 21 to 24, 2014, because they presented the most stable temperatures.

The temperatures evaluated correspond to the values of the maximum temperatures (Tmax), minimum temperatures (Tmin), mean temperature (Timed), and the thermal amplitudes of temperature presented on the outer and inner surface of each panel. **Figure 9** shows the evolution of the exterior surface temperature wave, while **Figure 10** shows the interior surface temperatures recorded. It is observed that the highest values of thermal amplitudes were presented in the exterior surface temperatures due to the direct exposure to solar radiation. It is observed that the highest exterior thermal amplitude was presented in the (PO + CE) specimen because it presented a very high surface temperature attributed to the panel's black color. Regarding the interior surface temperatures these were presented as follows:

$$(2F + POCE) < (PO + CE) < (2F + A) < (CLC) < (LF) \tag{2}$$

Table 4 summarizes the results of the thermal amplitudes obtained on the exterior and interior surfaces of the specimens. The decrement factor of the analyzed roof specimens is also presented. **Figure 10** shows the results for the interior thermal amplitudes, which were given as follows (2F + POCE) < (PO + CE) < (2F + A) < (CLC) < (LF). **Figure 11** shows the decrement factor from smallest to largest following the same pattern: (2F + POCE (0.19)) < (PO + CE (0.30)) < (2F + A (0.50)) < (CLC (0.73)) < (LF (1.06)), this indicates that the specimen (2F + POCE) achieves the lowest thermal decrement factor of external temperature waves.

Table 5 shows the comparative results of the average thermal lag obtained from the indoor surface temperatures concerning the outdoor surface temperatures of the roof systems under study. The average thermal lag values obtained from the 4 days of the experimental period (March 21 to 24) are presented from highest to lowest and were given as follows: (2F + POCE (6:03)) > (PO + CE (3:52)) > (2F + A
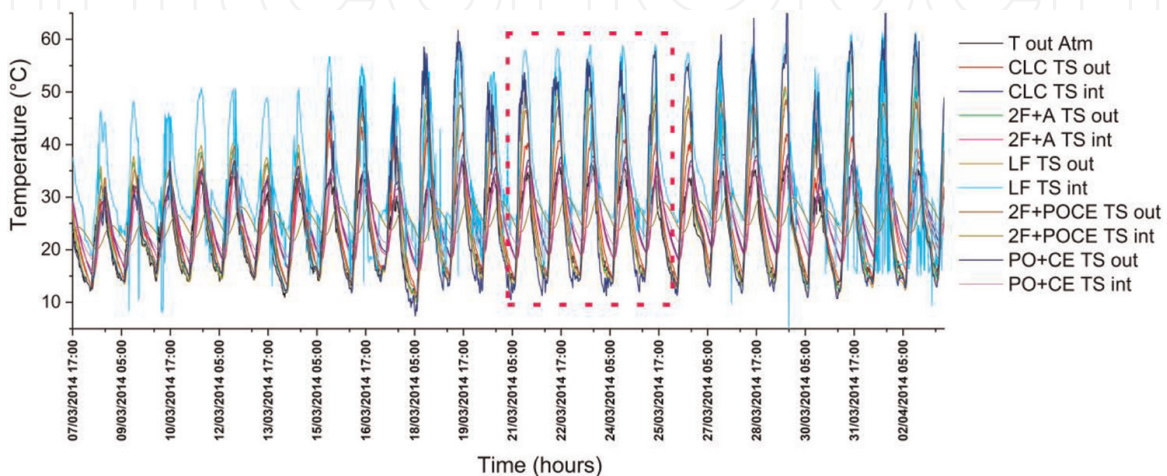

Figure 8.
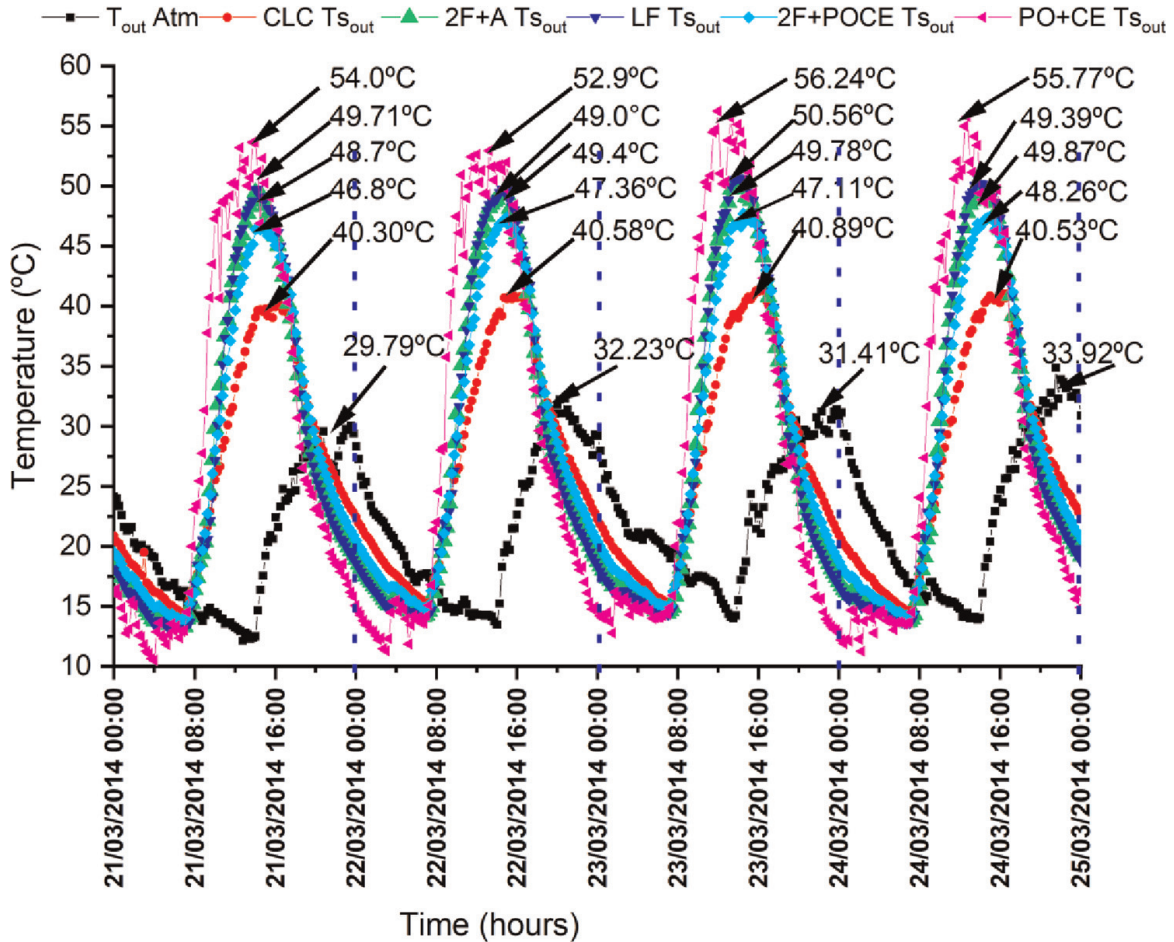*Indoor ambient + outdoor ambient temperatures (March 7 to April 3).*

Figure 9.
Thermal amplitudes based on outdoor surface temperature in (2F + POCE) vs. (PO + CE) vs. (2F + a) vs. (CLC) vs. (LF) roofs and outdoor ambient temperature.

(2:30)) > (CLC (0:30)) > (LF (0:15)). **Figure 12** exemplifies the thermal lag obtained for March 23. The results obtained from the average thermal lag indicate that the specimen (2F + POCE) achieves the highest thermal lag of the outside temperature waves (6,00 hours).

Belhadj et al. [56] investigated straw and cement walls with different thicknesses from 0.1 to 0.25 m reporting thermal lag values of 4 to 8 hr. and a decrement factor of 0.15 to 0.85. Panel 2F + POCE presented a thermal lag of 6:00 hrs and a decrement factor of 0.19. These values are thermally better than the compressed earth specimens by Roux-Gutiérrez and Velázquez-Lozano [57] with different types of plasters. The double block compressed earth without plaster recorded a thermal lag of 4:15 hrs and a decrement factor of 2.28. Other conventional materials such as baked mud brick or cement mortar block recorded thermal lag values of about 0:30 hr. and decrement factor values of about 1.88. Gallegos-Ortega et al. [58] studied a house with thatched walls of 0.4 m in width in Tecate, Baja California, Mexico. Their results showed a thermal lag of 9 to 12 hrs, which means 2 hrs above the 2F + POCE panel, influenced by the greater thickness of the specimen.

The control panel LF, made of ferrocement only, shows the lowest thermal lag and highest decrement factor compared to the other panels tested. CLC panel showed a thermal lag increment of 200% and decrement factor reduction of 31%; panel 2F + A had a thermal lag rise of 1000% and a decrement factor reduction of 52.8%; panel PO + CE had a thermal lag rise of 1360% and a decrement factor reduction of 71.7%. The proposed panel 2F + POCE showed a thermal lag increment of 2400% and a decrement factor reduction of 82%.
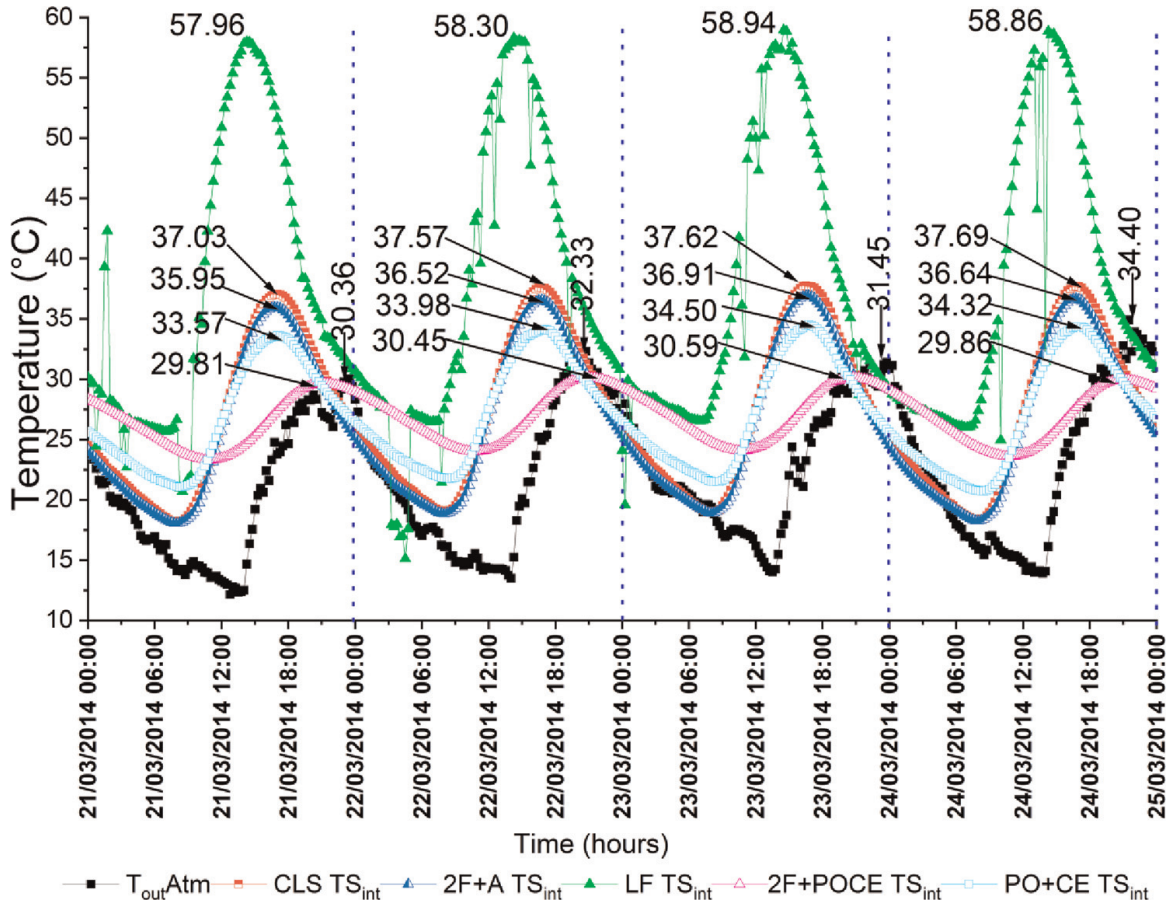
Figure 10.
Thermal amplitudes based on indoor surface temperature in (2F + POCE) vs. (PO + CE) vs. (2F + a) vs. (CLC) vs. (LF) roofs and outdoor ambient temperature.

Specimen	Outside surface temperature from March 21 to 24			Inside surface temperature from March 21 to 24			Decrement factor
	Temp Max (°C)	Temp Min (°C)	ΔT Outside surface	Temp Max (°C)	Temp Min (°C)	ΔT Inside surface	
LF	50.20	13.81	36.39	58.52	20.10	38.42	1.06
CLC	40.92	14.94	25.98	37.52	18.65	18.87	0.73
2F + A	49.68	13.89	35.79	36.53	18.52	18.01	0.50
PO + CE	54.66	11.47	43.20	34.12	21.27	12.86	0.30
2F + POCE	47.26	14.49	32.77	29.99	23.76	6.24	0.19

Table 4.
Thermal amplitude values and decrement factor of (2F + POCE) vs. (LF) vs. (CLC) vs. (2F + a) vs. (PO + CE).

Thus, the results obtained in this work with the proposed panel 2F + POCE indicate that it is a viable option for use in walls and roofs in warm and temperate climates with high thermal oscillations.

3.3 Results of thermal conductivity

In the conductivimeter, a heat flow of 32.4 watts was fed to the panel PO + CE. The thermal temperature in a steady state was monitored for 4 days. The mean thermal
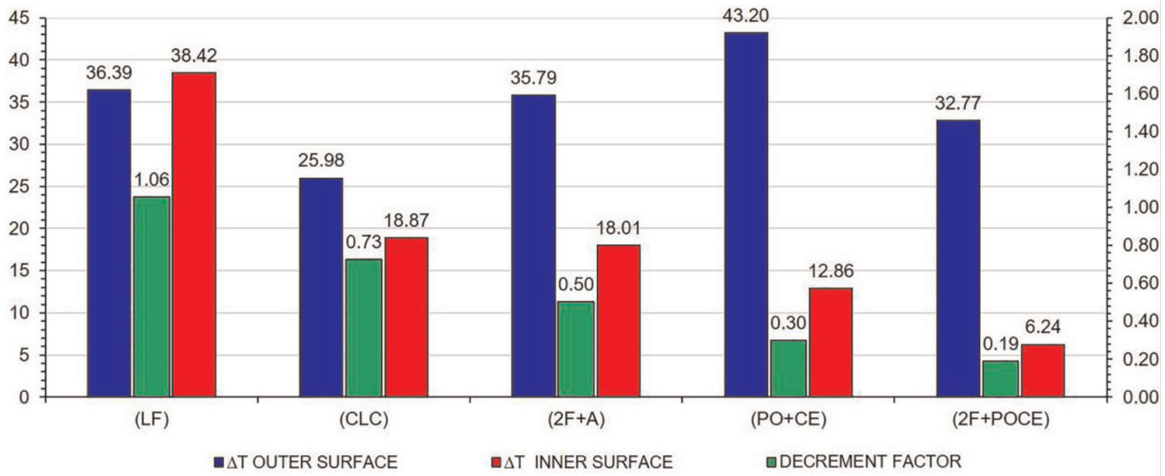
Figure 11.
Comparative results of the decrement factor in roofs: (2F + POCE) vs. (PO + CE) vs. (2F + a) vs. (CLC) vs. (LF).

Thermal lag mean from march 21–24, 2014					
Experimental cells	**21**	**22**	**23**	**24**	**Thermal Lag**
Sample 1 (2F + POCE)	6:15	6:00	6:00	6:00	6:03
Sample 2 (PO + CE)	3:00	3:45	4:45	4:00	3.52
Sample 3 (2F + A)	2:45	1:45	2:30	3:00	2:30
Sample 4 (CLC)	0:30	0:45	0:15	0:30	0:30
Sample 5 (LF)	0:00	0:15	0:30	0:30	0:15

Table 5.
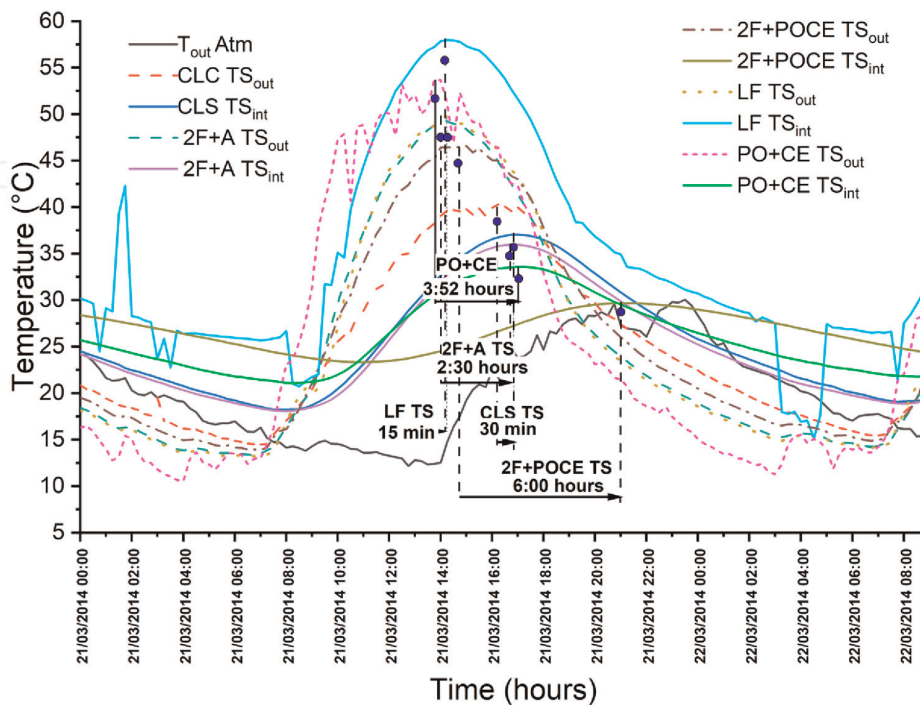*Comparative results of thermal lag in roofs.*

Figure 12.
Comparative results of thermal lag in roofs: (2F + POCE) vs. (PO + CE) vs. (2F + a) vs. (CLC) vs. (LF).

conductivity of panel PO + CE was 0.2008 ± 0.0064 W/m·K, Maximum 0.207 W/m·K, minimum 0.194 W/m·K, median 0.203 W/m·K.

Insulating materials have thermal conductivity values of 0.01 to 0.09 W/m K. Alavez-Ramirez et al. [55] found thermal conductivity values for ferrocement of 0.69 W/m K, ferrocement plus coconut fiber 0.221 W/m K, lightweight concrete brick 0.53 W/m K, hollow concrete block 0.68 W/m K and red clay brick 0.93 W/m K. Ruiz Torres et al. [59] reported thermal conductivity for thermos-slab 0.263 W/m K, cement-sand mortar 0.63 W/m K, typical annealed red brick 0.872 W/m K. Borbón Almada et al. [60] reported a thermal conductivity for annealed mud brick 0.814 W/m K, lightened block 0.465 W/m K, cement-sand mortar 0.470 W/m K and recycled cement-sand mortar 0.291 W/m K (recycled material from concrete demolition). Rico Rodríguez et al. [61] reported a value of 0.21 W/m K in the thermal conductivity of a cement composite material reinforced with bagasse ash and fiber. In this context, the thermal conductivity value of 0.2008 W/m·K of the PO + CE panel proposed in this study has a low thermal conductivity suitable for thermal applications in construction.

4. Conclusions

The bioclimatic analysis for the city of Oaxaca showed internal heating and thermal mass requirements for thermal comfort conditions. A hybrid panel composed of cane bagasse ash, corncob, and lime was proposed to reach such comfort conditions. A sandwich-type construction component was made with the hybrid panel and two outer layers of reinforced mortar (ferrocement) and the middle of the cane bagasse ash and corncob panel (2F + POCE). Five experimental chambers were built to determine the surface thermal performance of the panels (2F + POCE), (PO + CE), (2F + A), (CLC), and (LF). The month of March was selected for the analysis based on the climatic normals of the locality. The best decrement factor and thermal lag were presented in the panel consisting of two ferrocement slabs and the waffle panel (2F + POCE), registering 0.19 and 6 hrs, respectively. These results are significant because the panel limits the heat flow at peak hours when temperatures reach their highest values. Therefore, such a composite can provide an environmentally friendly alternative for energy savings and thermal comfort.

Acknowledgements

Conflict of interest

The authors declare that they have no known competing financial interests or personal relationships that could have appeared to influence the work reported in this work.

Author details

Rafael Alavéz-Ramírez[1], Fernando Chiñas-Castillo[2]*, Magdaleno Caballero-Caballero[1],
Valentín Juventino Morales-Domínguez[1], Margarito Ortiz-Guzmán[1],
Maria Eugenia Silva-Rivera[1], Roberto Candido Jimenez-Piñon[2]
and Angel Ramos-Alonso[2]

1 National Polytechnic Institute IPN, CIIDIR Oaxaca, Santa Cruz Xoxocotlán, Oaxaca,
México

2 Department of Mechanical Engineering, National Technological Institute of Mexico/
Oaxaca Institute of Technology, Oaxaca de Juarez, Oax, México

*Address all correspondence to: fernandochinas@gmail.com

IntechOpen

References

[1] Manzano-Agugliaro F, Montoya FG, Sabio-Ortega A, García-Cruz A. Review of bioclimatic architecture strategies for achieving thermal comfort. Renewable and Sustainable Energy Reviews. 2015;**49**: 736-755. DOI: 10.1016/j.rser.2015.04.095

[2] Wegertseder P, Schmidt D, Hatt T, Saelzer G, Hempel R. Barreras y oportunidades observadas en la incorporación de estándares de alta eficiencia energética en la vivienda social chilena. Arquit y Urban. 2014;**XXXV**: 37-49

[3] Ofori G, Briffett C IV, Gang G, Ranasinghe M. Impact of ISO 14000 on construction enterprises in Singapore. Construction Management and Economics. 2000;**18**:935-947. DOI: 10.1080/014461900446894

[4] Gino Moncada LG, Asdrubali F, Rotili A. Influence of new factors on global energy prospects in the medium term: Comparison among the 2010, 2011 and 2012 editions of the IEA's world energy outlook reports. Economics and Policy of Energy Environment. 2013;**3**: 67-89. DOI: 10.3280/EFE2013-003003

[5] Zhang Y, Wang J, Hu F, Wang Y. Comparison of evaluation standards for green building in China, Britain, United States. Renewable and Sustainable Energy Reviews. 2017;**68**:262-271. DOI: 10.1016/J.RSER.2016.09.139

[6] WBCSD. Energy Efficiency in Buildings Facts and Trends: Business Realities and Opportunities. Switzerland: WBCSD. July 2008. ISBN: 978-3-940388-26-1

[7] Bressand F, Farrell D, Haas P, Morin F. Curbing Global Energy Demand Growth: The Energy Productivity Opportunity. McKinsey Glob Inst. Sao Paulo, Brazil: McKinsey&Company. 2007. pp. 1-290

[8] Secretaria del Medio Ambiente del Gobierno del Distrito Federal. Gac Of Del Dist Fed: Programa de certificación de edificaciones sustentables; 2012. pp. 1-90

[9] Mounir S, Khabbazi A, Khaldoun A, Maaloufa Y, El Hamdouni Y. Thermal inertia and thermal properties of the composite material clay-wool. Sustainable Cities and Society. 2015;**19**: 191-199. DOI: 10.1016/j.scs.2015.07.018

[10] Wang L, Zhou Q, Ji X, Peng J, Nawaz H, Xia G, et al. Fabrication and characterization of transparent and uniform cellulose/polyethylene composite films from used disposable paper cups by the "one-pot method.". Polymers (Basel). 2022;**14**:1070-1085. DOI: 10.3390/polym14061070

[11] Soret GM, Vacca P, Tignard J, Hidalgo JP, Maluk C, Aitchison M, et al. Thermal inertia as an integrative parameter for building performance. Journal of Building Engineering. 2021;**33**: 101623. DOI: 10.1016/j.jobe.2020.101623

[12] Chikhi M. Young's modulus and thermophysical performances of bio-sourced materials based on date palm fibers. Energy and Buildings. 2016;**129**: 589-597. DOI: 10.1016/j.enbuild.2016.08.034

[13] Çomak B, Bideci A, Salli BÖ. Effects of hemp fibers on characteristics of cement based mortar. Construction and Building Materials. 2018;**169**:794-799. DOI: 10.1016/j.conbuildmat.2018.03.029

[14] Hamza S, Saad H, Charrier B, Ayed N, Charrier-El BF. Physico-chemical characterization of Tunisian

plant fibers and its utilization as reinforcement for plaster based composites. Industrial Crops and Products. 2013;**49**:357-365. DOI: 10.1016/j.indcrop.2013.04.052

[15] Cherki AB, Remy B, Khabbazi A, Jannot Y, Baillis D. Experimental thermal properties characterization of insulating cork-gypsum composite. Construction and Building Materials. 2014;**54**:202-209. DOI: 10.1016/j. conbuildmat.2013.12.076

[16] Khalil A, Khalil HPSA, Alwani MS, Mohd Omar AK. Chemical composition, anatomy, lignin distribution, and cell wall structure of Malaysian plant waste fibers. BioResources. 2006;**1**:220-232

[17] Loh YR, Sujan D, Rahman ME, Das CA. Sugarcane bagasse—The future composite material: A literature review. Resources, Conservation and Recycling. 2013;**75**:14-22. DOI: 10.1016/J. RESCONREC.2013.03.002

[18] Manohar K. Experimental investigation of building thermal insulation from agricultural by-products. British Journal of Applied Science and Technology. 2012;**2**:227-239. DOI: 10.9734/bjast/2012/1528

[19] Aminudin E, Khalid NHA, Azman NA, Bakri K, Din MFM, Zakaria R, et al. Utilization of Baggase waste based materials as improvement for thermal insulation of cement brick. MATEC Web Conf. 2017;**103**: 01019. DOI: 10.1051/matecconf/2017 10301019

[20] Canilha L, Chandel AK, Suzane Dos Santos Milessi T, Antunes FAF, Luiz Da Costa Freitas W, Das Graças Almeida Felipe M, et al. Bioconversion of sugarcane biomass into ethanol: An overview about composition, pretreatment methods, detoxification of hydrolysates, enzymatic saccharification, and ethanol fermentation. Journal of Biomedicine & Biotechnology. 2012;**2012**: 2012. DOI: 10.1155/2012/989572

[21] Watt JD, Thorne DJ. Composition and pozzolanic properties of pulverised fuel ashes.* I. composition of fly ashes from some component particles British power stations and properties of their component particles. Journal of Applied Chemistry. 1965;**15**:585-594

[22] Moraes JCB, Melges JLP, Akasaki JL, Tashima MM, Soriano L, Monzó J, et al. Pozzolanic reactivity studies on a biomass-derived waste from sugar cane production: Sugar cane straw ash (SCSA). ACS Sustainable Chemistry & Engineering. 2016;**4**:4273-4279. DOI: 10.1021/acssuschemeng.6b00770

[23] Payá J, Monzó J, Borrachero MV, Díaz-Pinzón L, Ordónez LM. Sugar-cane bagasse ash (SCBA): Studies on its properties for reusing in concrete production. Journal of Chemical Technology and Biotechnology. 2002;**77**: 321-325. DOI: 10.1002/jctb.549

[24] Neville AM. Tecnología del concreto: Curado del concreto. Mexico D.F: Instituto Mexicano del Cemento y del Concreto, A. C; 2013

[25] Martirena Hernandez JF, Middendorf B, Gehrke M, Budelmannt H. Use of wastes of the sugar industry as pozzolana in lime-pozzolana binders: Study of the reaction. Cement and Concrete Research. 1998;**28**: 1525-1536. DOI: 10.1016/S0008-8846 (98)00130-6

[26] Cordeiro GC, Toledo Filho RD, Tavares LM, Fairbairn EMR. Pozzolanic activity and filler effect of sugar cane bagasse ash in Portland cement and lime mortars. Cement and Concrete Composites. 2008;**30**:410-418.

DOI: 10.1016/J.CEMCONCOMP.2008.
01.001

[27] Cordeiro GC, Toledo Filho RD, Fairbairn EMR. Effect of calcination temperature on the pozzolanic activity of sugar cane bagasse ash. Construction and Building Materials. 2009;**23**: 3301-3303. DOI: 10.1016/J. CONBUILDMAT.2009.02.013

[28] Ganesan K, Rajagopal K, Thangavel K. Evaluation of bagasse ash as supplementary cementitious material. Cement and Concrete Composites. 2007; **29**:515-524. DOI: 10.1016/J. CEMCONCOMP.2007.03.001

[29] Jauberthie R, Rendell F, Tamba S, Cisse I. Origin of the pozzolanic effect of rice husks. Construction and Building Materials. 2000;**14**:419-423. DOI: 10.1016/S0950-0618(00)00045-3

[30] Chandrasekhar S, Satyanarayana KG, Pramada PN, Raghavan P, Gupta TN. Processing, properties and applications of reactive silica from rice husk-an overview. Journal of Materials Science. 2003;**38**: 3159-3168

[31] Chandrasekhar S, Pramada PN, Majeed J. Effect of calcination temperature and heating rate on the optical properties and reactivity of rice husk ash. Journal of Materials Science. 2006;**41**:7926-7933. DOI: 10.1007/ s10853-006-0859-0

[32] Frías M, Villar-Cociña E, De Rojas MIS, Valencia-Morales E. The effect that different pozzolanic activity methods has on the kinetic constants of the pozzolanic reaction in sugar cane straw-clay ash/lime systems: Application of a kinetic–diffusive model. Cement and Concrete Research. 2005;**35**: 2137-2142. DOI: 10.1016/J. CEMCONRES.2005.07.005

[33] Wu N, Ji T, Huang P, Fu T, Zheng X, Xu Q. Use of sugar cane bagasse ash in ultra-high performance concrete (UHPC) as cement replacement. Construction and Building Materials. 2022;**317**:125881. DOI: 10.1016/J. CONBUILDMAT.2021.125881

[34] Yadav AL, Sairam V, Srinivasan K, Muruganandam L. Synthesis and characterization of geopolymer from metakaolin and sugarcane bagasse ash. Construction and Building Materials. 2020;**258**:119231. DOI: 10.1016/J. CONBUILDMAT.2020.119231

[35] Mehrzad S, Taban E, Soltani P, Samaei SE, Khavanin A. Sugarcane bagasse waste fibers as novel thermal insulation and sound-absorbing materials for application in sustainable buildings. Building and Environment. 2022;**211**:108753. DOI: 10.1016/J. BUILDENV.2022.108753

[36] Brito FMS, Bortoletto Júnior G, Paes JB, Belini UL, Tomazello-Filho M. Technological characterization of particleboards made with sugarcane bagasse and bamboo culm particles. Construction and Building Materials. 2020;**262**:120501. DOI: 10.1016/J. CONBUILDMAT.2020.120501

[37] Gharieb M, Rashad AM. An initial study of using sugar-beet waste as a cementitious material. Construction and Building Materials. 2020;**250**:118843. DOI: 10.1016/J.CONBUILDMAT.2020. 118843

[38] Jagadesh P, Ramachandra Murthy A, Murugesan R. Effect of processed sugar cane bagasse ash on mechanical and fracture properties of blended mortar. Construction and Building Materials. 2020;**262**:120846. DOI: 10.1016/J. CONBUILDMAT.2020.120846

[39] Jittin V, Bahurudeen A. Evaluation of rheological and durability

characteristics of sugarcane bagasse ash and rice husk ash based binary and ternary cementitious system. Construction and Building Materials. 2022;**317**:125965. DOI: 10.1016/J. CONBUILDMAT.2021.125965

[40] Tripathy A, Acharya PK. Characterization of bagasse ash and its sustainable use in concrete as a supplementary binder – A review. Construction and Building Materials. 2022;**322**:126391. DOI: 10.1016/J. CONBUILDMAT.2022.126391

[41] Souza NSL de, Anjos MAS dos, Sá M, de Das VVA, de Farias EC, de Souza MM, Branco FG, et al, Evaluation of sugarcane bagasse ash for lightweight aggregates production. Construction and Building Materials 2021;271:121604. doi: 10.1016/J.CONBUILDMAT.2020. 121604

[42] Subedi S, Arce GA, Hassan MM, Barbato M, Mohammad LN, Rupnow T. Feasibility of ECC with high contents of post-processed bagasse ash as partial cement replacement. Construction and Building Materials. 2022;**319**:126023. DOI: 10.1016/J. CONBUILDMAT.2021.126023

[43] Klathae T, Tanawuttiphong N, Tangchirapat W, Chindaprasirt P, Sukontasukkul P, Jaturapitakkul C. Heat evolution, strengths, and drying shrinkage of concrete containing high volume ground bagasse ash with different LOIs. Construction and Building Materials. 2020;**258**:119443. DOI: 10.1016/J.CONBUILDMAT. 2020.119443

[44] Klathae T, Tran TNH, Men S, Jaturapitakkul C, Tangchirapat W. Strength, chloride resistance, and water permeability of high volume sugarcane bagasse ash high strength concrete incorporating limestone powder.

Construction and Building Materials. 2021;**311**:125326. DOI: 10.1016/J. CONBUILDMAT.2021.125326

[45] Barbosa FL, Cordeiro GC. Partial cement replacement by different sugar cane bagasse ashes: Hydration-related properties, compressive strength and autogenous shrinkage. Construction and Building Materials. 2021;**272**:121625. DOI: 10.1016/J.CONBUILDMAT.2020. 121625

[46] Athira G, Bahurudeen A. Rheological properties of cement paste blended with sugarcane bagasse ash and rice straw ash. Construction and Building Materials. 2022;**332**:127377. DOI: 10.1016/J.CONBUILDMAT.2022. 127377

[47] Fuentes FV. Mapas bioclimáticos de la República Mexicana. 1a. ed. México D. F: Universidad Autónoma Metropolitana; 2014

[48] Köppen WP. Climatologia, con un estudio de los climas de la tierra. Mexico D.F: Mexico, Fondo de Cultura Economica; 1948

[49] Garcia E. Modificaciones al sistema de clasificacion climatica de Koppen. 2004th ed. Mexico D.F: Instituto de Geografia UNAM; 2004

[50] Carvalho W, Canilha L, Castro PF, Barbosa LDFO. Chemical composition of the sugarcane bagasse. In: Society for Industrial Microbiology, Editor. 31st Symp. Biotechnol. Fuels Chem. Society for Industrial Microbiology: San Francisco CA; 2015

[51] Luz SM, Gonçalves AR, Ferrão PMC, Freitas MJM, Leão AL, Del Arco AP Jr. Water absorption studies of vegetable fibers reinforced polypropylene composites. In: Proceeding of 6th Int. Symp. Nat. Polym. Compos. ISNaPol 6

and XI International Macromolecular Colloquium IMC 11. Gramado, RS Brazil: Associacao Brasileira de Polimeros (ABPol); 22-25 April, 2007. pp. 73-78

[52] Ramlee NA, Naveen J, Jawaid M. Potential of oil palm empty fruit bunch (OPEFB) and sugarcane bagasse fibers for thermal insulation application – A review. Construction and Building Materials. 2021; **271**:121519. DOI: 10.1016/J.CONBUILD MAT.2020.121519

[53] Alavéz-Ramírez R, Chiñas-Castillo F, Morales-Domínguez VJ, Ortiz-Guzmán M, Caballero-Montes JL, Caballero-Caballero M. Thermal lag and decrement factor of constructive component reinforced mortar channels filled with soil–cement–sawdust. Indoor and Built Environment. 2018;**27**: 466-485. DOI: 10.1177/ 1420326X16676611

[54] Alavéz Ramírez R, Morales Domínguez VJ, Ortiz GM. Mortero a base de Olote, ceniza de bagazo de caña y cal como relleno ligero. 6to. Congr. Int. Virtual Innovación Tecnológica y Educ. Ediciones ILCSA S.A. de C.V: CIVITEC, Tijuana, Baja California, México; 2018

[55] Alavez-Ramirez R, Chiñas-Castillo F, Morales-Dominguez VJ, Ortiz-Guzman M. Thermal conductivity of coconut fibre filled ferrocement sandwich panels. Construction and Building Materials. 2012;**37**:425-431. DOI: 10.1016/j. conbuildmat.2012.07.053

[56] Belhadj B, Bederina M, Makhloufi Z, Goullieux A, Quéneudec M. Study of the thermal performances of an exterior wall of barley straw sand concrete in an arid environment. Energy and Buildings. 2015;**87**:166-175. DOI: 10.1016/j. enbuild.2014.11.034

[57] Roux-Gutiérrez RS, Velázquez LJ. Bloques de Tierra Comprimida, Su

Retardo Térmico e Impacto Ambiental. Rev Legado Arquit y Diseño. Mexico: Universidad Autónoma del Estado de Mexico; 2016. pp. 1-13. ISSN: 2448-749X

[58] Gallegos-Ortega R, Magaña-Guzmán T, Reyes-López JA, Romero-Hernández MS. Thermal behavior of a straw bale building from data obtained in situ. A case in northwestern México. Building and Environment. 2017;**124**: 336-341. DOI: 10.1016/j. buildenv.2017.08.015

[59] Ruiz Torres RP. Evaluación del Sistema Termolosa entre la medición experimental y el calculado con la NMX-C-460-ONNCCE-2009. Vivienda y Comunidades Sustentables. 2019;**2019**: 119-136. DOI: 10.32870/rvcs.v0i6.126

[60] Borbón Almada AC, Alpuche Cruz MG, Miranda Pasos I, Marincic Lovriha I, Ochoa de la Torre JM. Materiales reciclados aligerados y su influencia en el consumo de energía eléctrica en viviendas económicas. Acta Univ. 2019;**29**:1-15. DOI: 10.15174/ au.2019.2096

[61] Rico Rodríguez I, Vargas Galarza Z, García Hernández E, Salgado Delgado R, Cárdenas Valdez RC, Olarte PA. Evaluación térmica de material compuesto de cemento portland reforzado con agregado fino de CBC y FO tratada con Silano. Ing Investig y Tecnol. 2020;**21**:1-11. DOI: 10.22201/ fi.25940732e.2020.21n1.001